Applied and Environmental Microbiology

Diversity, Abundance, and Potential Activity of Nitrifying and Nitrate-Reducing Microbial Assemblages in a Subglacial Ecosystem

Eric S. Boyd, Rachel K. Lange, Andrew C. Mitchell, Jeff R. Havig, Trinity L. Hamilton, Melissa J. Lafrenière, Everett L. Shock, John W. Peters and Mark Skidmore

Appl. Environ. Microbiol. **2011, 77(14):4778. DOI: 10.1128/AEM.00376-11.**
Published Ahead of Print 27 May 2011.

Applied and Environmental Microbiology, July 2011, p. 4778–4787 Vol. 77, No. 14
0099-2240/11/$12.00 doi:10.1128/AEM.00376-11

Diversity, Abundance, and Potential Activity of Nitrifying and Nitrate-Reducing Microbial Assemblages in a Subglacial Ecosystem▽†

Eric S. Boyd,[1]* Rachel K. Lange,[1]‡ Andrew C. Mitchell,[2]§ Jeff R. Havig,[3] Trinity L. Hamilton,[1] Melissa J. Lafrenière,[4] Everett L. Shock,[3,5] John W. Peters,[1] and Mark Skidmore[6]

Department of Chemistry and Biochemistry and the Astrobiology Biogeocatalysis Research Center, Montana State University, Bozeman, Montana 59717[1]; Center for Biofilm Engineering, Montana State University, Bozeman, Montana 59717[2]; School of Earth and Space Exploration, Arizona State University, Tempe, Arizona 85287[3]; Department of Geography, Queen's University, Kingston, Ontario K7L 3N6, Canada[4]; Department of Chemistry and Biochemistry, Arizona State University, Tempe, Arizona 85287[5]; and Department of Earth Sciences, Montana State University, Bozeman, Montana 59717[6]

Received 18 February 2011/Accepted 3 May 2011

Subglacial sediments sampled from beneath Robertson Glacier (RG), Alberta, Canada, were shown to harbor diverse assemblages of potential nitrifiers, nitrate reducers, and diazotrophs, as assessed by *amoA*, *narG*, and *nifH* gene biomarker diversity. Although archaeal *amoA* genes were detected, they were less abundant and less diverse than bacterial *amoA*, suggesting that bacteria are the predominant nitrifiers in RG sediments. Maximum nitrification and nitrate reduction rates in microcosms incubated at 4°C were 280 and 18.5 nmol of N per g of dry weight sediment per day, respectively, indicating the potential for these processes to occur *in situ*. Geochemical analyses of subglacial sediment pore waters and bulk subglacial meltwaters revealed low concentrations of inorganic and organic nitrogen compounds. These data, when coupled with a C/N atomic ratio of dissolved organic matter in subglacial pore waters of ~210, indicate that the sediment communities are N limited. This may reflect the combined biological activities of organic N mineralization, nitrification, and nitrate reduction. Despite evidence of N limitation and the detection of *nifH*, we were unable to detect biological nitrogen fixation activity in subglacial sediments. Collectively, the results presented here suggest a role for nitrification and nitrate reduction in sustaining microbial life in subglacial environments. Considering that ice currently covers 11% of the terrestrial landmass and has covered significantly greater portions of Earth at times in the past, the demonstration of nitrification and nitrate reduction in subglacial environments furthers our understanding of the potential for these environments to contribute to global biogeochemical cycles on glacial-interglacial timescales.

Abundant, diverse, and metabolically active microbial populations are now known to inhabit the subglacial environments of Earth's glaciers and larger ice masses, despite persistent cold temperatures of 0 to 1°C (12, 16, 28, 50, 51). These microbial populations are thought to be supported largely through redox reactions that are often accompanied by the weathering of the local bedrock (48, 50, 58) and that may have important implications for global biogeochemical cycles on glacial-interglacial timescales (1, 9, 54, 60). Consequently, the metabolisms supporting these cold-adapted populations and their contributions to local and global biogeochemical cycles have been the subject of investigation for the past decade (16, 48, 51, 54).

Recent evidence suggests the presence of microbial populations in subglacial environments that are likely supported by redox transformations of nitrogenous compounds. For example, *ex situ* microcosms containing subglacial sediment sampled from the base of John Evans Glacier, Canada (51), and from the base of Fox Glacier and Franz Josef Glacier, New Zealand (16), were shown to consume nitrate (NO_3^-) when incubated anaerobically at 4°C although it is unclear if the NO_3^- was assimilated (assimilatory nitrate reduction) or if the NO_3^- was utilized as an electron acceptor during respiration (respiratory denitrification). The first step in denitrification is the reduction of NO_3^- to nitrite (NO_2^-) (e.g., nitrate reduction) which occurs via the activity of either periplasmic or cytoplasmic nitrate reductases (encoded by *napAB* and *narGHI*, respectively) (44, 66). In respiratory denitrification, NO_2^- is sequentially reduced to dinitrogen (N_2) via nitric oxide (NO) and nitrous oxide (N_2O) (66). Denitrification is widely distributed among a polyphyletic group of bacteria and archaea (42, 66). Consequently, small-subunit (SSU) rRNA gene primers are of little use in characterizing the diversity of populations involved in denitrification pathways (43, 52). Thus, primers targeting *narG* (43) and *napA* (15) genes have been specifically developed to characterize the diversity of nitrate-reducing populations in natural environments.

Geochemical and isotopic analyses of subglacial meltwaters

* Corresponding author. Mailing address: Department of Chemistry and Biochemistry, 103 Chemistry Research Building, Montana State University, Bozeman, MT 59717. Phone: (406) 994-7213. Fax: (406) 994-5407. E-mail: eboyd@montana.edu.

‡ Present Address: School of Aquatic and Fishery Science, University of Washington, Seattle, WA 98195.

§ Present Address: Institute of Geography and Earth Sciences, Aberystwyth University, Ceredigion SY23 3DB, United Kingdom.

† Supplemental material for this article may be found at http://aem.asm.org/.

▽ Published ahead of print on 27 May 2011.

sampled from Arctic glacial systems (Midtre Lovénbreen and Austre Brøggerbreen, Svalbard, Norway) are also suggestive of NO_3^- production in the subglacial environment during an annual glacial meltcycle (21, 62). The source of the NO_3^- produced in the subglacial system was hypothesized to be the result of the mineralization of organic nitrogen (N) with subsequent oxidation of released ammonium (NH_4^+) to NO_3^- (62). Nitrification or the sequential oxidation of NH_4^+ to NO_3^- via NO_2^- links the mineralization of nitrogenous organic matter to N loss from a system via denitrification (sequential reduction of NO_3^- to N_2 gas) (66). The rate-limiting step in nitrification (the oxidation of NH_4^+ to NH_2OH) is catalyzed by a suite of phylogenetically distinct lineages of *Beta-* and *Gammaproteobacteria* and in several lineages of *Thaumarchaeota* by the ammonia monooxygenase (AMO) (17, 30, 45). These organisms couple the oxidation of NH_4^+ to the reduction of CO_2 and, thus, have an impact on both the nitrogen and carbon cycles (30, 61). Primers targeting the *amoA* gene have been used to characterize the distribution, diversity, and abundance of ammonia-oxidizing bacteria (AOB) and ammonia-oxidizing archaea (AOA) in a variety of marine (36, 61), freshwater (45), and terrestrial environments (32, 59). These studies and others reveal the widespread distribution of terrestrial and marine bacteria and *Thaumarchaeota* that are likely to be involved in nitrification and have provided compelling evidence supporting their central role in the global nitrogen cycle.

Additional evidence for a subglacial biological nitrogen cycle comes from a recent examination of organic C and organic N in sediments collected from beneath Robertson Glacier (RG), Canada (9), which is underlain by a Devonian age sedimentary sequence consisting primarily of limestones, dolostones, and dolomitic limestones, with interbeds of shale, siltstone, and sandstone (35). The atomic ratio of particulate organic C to particulate organic N in RG sediment was ~137, which is similar to organic C/N ratios in kerogen and cherts deposited during the Precambrian (2, 19) but which is elevated compared to organic C/N ratios of 10 to 20 commonly observed in shales deposited during the Devonian period in other parts of North America (24). Elevated organic C/N ratios, such as those observed in RG sediments, are thought to reflect preferential mineralization of organic N in particulate matter relative to organic C during diagenesis (2, 19) although it is unknown if the elevated ratio in RG sediments reflects historical diagenesis of the shale (the likely source rock for the organic C and N in the sediments) or contemporary organic N mineralization followed by nitrification and denitrification.

Despite multiple independent lines of evidence suggesting the potential for microbially mediated nitrification and nitrate reduction in subglacial environments (9, 16, 21, 51, 62), the diversity, abundance, and activity of microbial populations likely to be involved in these functional processes are not known. Here, we report the distribution, diversity, abundance, and activity potentials of microbial assemblages likely to be supported by nitrification and nitrate reduction reactions in the subglacial environment at Robertson Glacier, Canada. These results are complemented by geochemical analyses of subglacial meltwaters and subglacial sediment pore waters (PW). Together, the results suggest the presence of an active biological N cycle in subglacial sediments and indicate that the microbial communities in the subglacial sediments are a sink for N in the subglacial environment. These results highlight a potential role for microbial activity in the loss of N from the subglacial environment and may help explain the elevated C/N ratios observed in dissolved organic matter sampled from subglacial pore waters and the organic matter in subglacial sediments.

MATERIALS AND METHODS

Field site description. Robertson Glacier (115°20′W, 50°44′N) drains the northern flank of the Haig Icefield in Peter Lougheed Provincial Park, Kananaskis Country, Alberta, Canada. The glacier is approximately 2 km long, spans an elevation range from 2,370 to 2,900 m, and currently terminates on a flat till plain although glacially smoothed bedrock surfaces are exposed along the glacier margins. Two principal subglacial meltwater streams (RG eastern drainage [RE] and RG western drainage [RW]) (Fig. 1) drain from beneath the ice front. The local bedrock is Upper Devonian in age (Mount Hawk, Palliser, and Sassenach Formations) and consists of impure limestones, dolostones, and dolomitic limestones, with interbeds of shale, siltstone, and sandstone (35, 47). A detailed description of the hydrology, geology, and subglacial melt water geochemistry for RG was reported previously (47).

Sample collection. Fine-grained basal sediments were collected from RE and RW at approximately 11:00 am on 9 July 2008, as previously described (6), for use in DNA-based analyses, pore water chemistry determinations, and microcosm experiments. Briefly, sediments were collected from the terminus of the glacier where RE and RW drainages emanate (Fig. 1), such that the sediments could be collected from beneath the ice. Two separate sediment samples from both RE and RW were collected using a flame-sterilized spatula. Sediments were placed in sterile 1.5-ml microcentrifuge tubes (DNA-based analyses) or sterile 250-ml polypropylene bottles (microcosm-based analyses and sediment pore water chemistry analyses) and were immediately flash frozen using a dry ice-ethanol slurry for transport back to the field station where they were kept frozen at −20°C. The frozen samples were transported on dry ice to Montana State University (MSU), where they were stored at −80°C until further processed. The dry solid content of the subglacial sediments sampled from RE and RW drainages, as determined by drying at 80°C for 24 h, was approximately 0.82 g of dry weight per gram of wet weight sediment.

Sediment pore water chemistry. Thawed sediment sampled at ~11:00 am on 9 July 2008 from RE (Fig. 1) was centrifuged (14,000 × *g* for 15 min at 4°C) in sterile microcentrifuge bottles, and the supernatant (pore water) was collected using a sterile pipette and filtered using 0.22-μm-pore-size nylon syringe filters. Concentrations of pore water-dissolved organic carbon and organic nitrogen were determined using a TOC-V (where TOC is total organic carbon) combustion analyzer equipped with a TMN1 analyzer (Shimadzu, Columbia, MD). Major cation concentrations were determined using a model 7500ce inductively coupled plasma mass spectrometer (Agilent, Palo Alto, CA) while anions (Fl^-, Cl^-, and SO_4^{2-}) were determined using an ion chromatography (IC) unit (Metrohm USA, Riverview, FL) equipped with a Metrosep A-2-250 analytical column (Metrohm USA). The concentrations of NH_4^+, NO_2^-, and NO_3^- were determined using a model MT-3 segmented flow analyzer (SEALQuAAtro, West Sussex, England) calibrated daily with freshly prepared standards.

Bulk meltwater geochemistry. Bulk meltwaters were collected from RE at 11:15 am and from RW at 2:00 pm on 9 July 2008. Meltwater samples were collected in opaque high-density polyethylene (HDPE) bottles and filtered immediately in the field. pH and electrical conductivity were measured in the field by using an Orion 4 Star pH/conductivity meter and probes (ThermoScientific) designed for low-ionic-strength solutions. Aliquots for analysis of dissolved ions were filtered through 0.22-μm-pore-size polyvinylidene fluoride (PVDF) filters and stored on ice in plastic scintillation vials without headspace. Aliquots were vacuum filtered through precombusted glass fiber filters (GF/F) for analysis of dissolved organic carbon (DOC) and total dissolved nitrogen (TDN). This filtrate was collected in 40-ml amber glass vials with Teflon-lined septa and acidified to a pH of ~2.0 with concentrated HCl.

Dissolved inorganic anions and cations (Cl^-, SO_4^{2-}, NO_3^-, Na^+, K^+, NH_4^+, Mg^{2+}, and Ca^{2+}) were measured using a Dionex 3000 ICS ion chromatography system (Dionex, Sunnyvale, CA) equipped with AS18 analytical and guard columns for anions and with CS12A analytical and guard columns for cations. Quantification of cations and anions was performed using certified standards (Dionex Seven Anion I and Dionex Six Cation II). DOC and TDN were analyzed by high-temperature combustion using a TOC-VPCH combustion analyzer

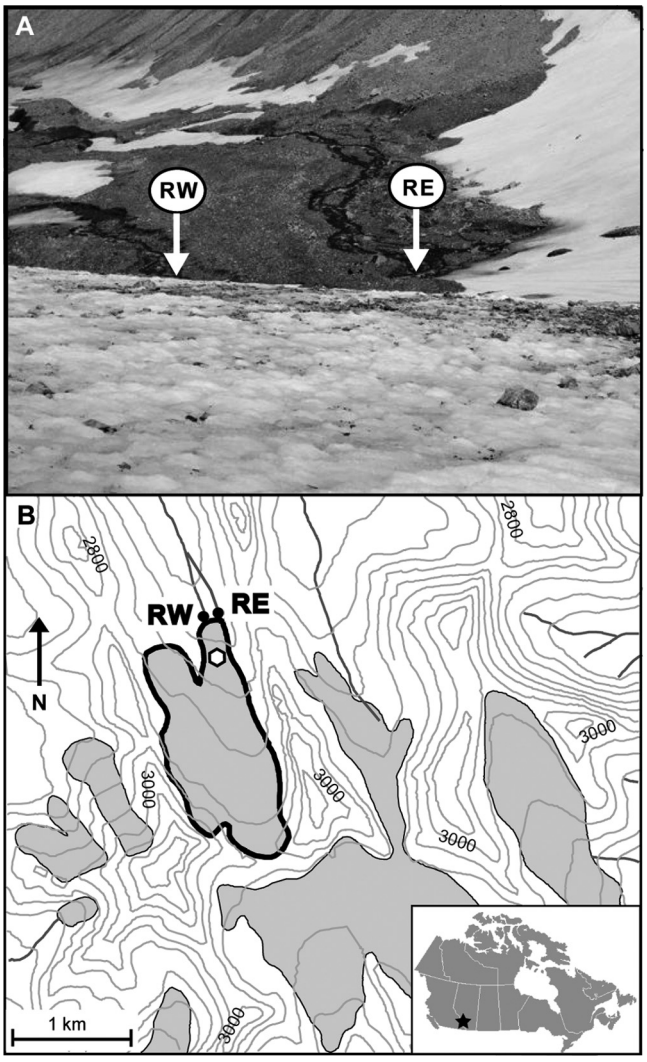

FIG. 1. Location map of Robertson Glacier. (A) Photograph of the glacier terminus highlighting the subglacial meltwater and sediment sampling sites from subglacial stream drainages RW and RE. The distance between the two outlet streams at the terminus is ~50 m. The photograph is taken looking down-glacier from the location on RG indicated by the hexagon on panel B. Sampling sites in this July 2008 image roughly correspond to sampling sites in September 2009; however, the latter sampling locations would be a short distance up-valley in response to the glacier retreat. (B) Topographic map of RG showing the stream sampling locations RW and RE. Gray-shaded areas are glaciers, with RG outlined in bold. Contour interval is 100 m. The inset image (bottom right) indicates the location of RG (star) within Alberta, Canada. The base map was prepared from National Topographic System (NTS) 1:50,000 maps 82J/14 and 82J/11 (© Department of Natural Resources Canada. All rights reserved).

equipped with a TMN1 analyzer (Shimadzu, Columbia, MD) and high-sensitivity catalyst. Dissolved organic nitrogen (DON) was calculated by subtracting the inorganic N species concentrations (NO_3^- and NH_4^+) from ion chromatography from the TDN obtained by high-temperature combustion.

Additional bulk meltwater samples and subglacial sediments from RE and RW were taken at ~12:00 pm on 14 September 2009 for geochemical and DNA-based analyses, respectively. This second sample set provided an opportunity for an initial assessment of interannual variability in certain microbial and geochemical parameters. pH and temperature were measured with a WTW 330i meter and probe, and conductivity and temperature were measured with a YSI 30 conductivity meter. Dissolved oxygen was measured with an AccuVac Ampule using a Hach DR/2400 Portable Spectrometer. Alkalinity was determined using a Hach Digital Titrator. Water was filtered using 0.8/0.2-μm-pore-size Supor syringe filters (Acrodisc 32-mm PF Syringe Filter with 0.8/0.2-μm Supor membrane) and collected after the filters were flushed with 20 ml of sample to minimize contamination. Aliquots used for analysis of DOC were collected in 40-ml amber borosilicate vials with silicone Teflon-lined septa and combined with 1 ml of concentrated H_3PO_4. Sample vials were filled to minimize headspace and sealed to minimize degassing and atmospheric contamination. DOC concentrations were measured with an OI Analytical Model 1010 Wet Oxidation TOC Analyzer, and CO_2 was obtained for quantification following the reaction of sample DOC with sodium persulfate. Samples for ion chromatography analysis of major cations (Dionex DX 120 IC System) and anions (Dionex DX 600 Dual IC System) were stored in 60-ml Nalgene bottles or 50-ml centrifuge tubes. Quantification of cations and anions was performed using certified standards (Alltech Multicomponent Certified Anion Standard Mix 6 and Dionex Combined 6 Cations Standard II). Standard deviations for IC values are based upon duplicate analyses. A field blank (18.2 MΩ deionized water transported to the field in a 1-liter Nalgene bottle) was taken using the same equipment and techniques described above.

Nitrification potential assays. The sediment pore water chemistry of samples collected in July 2008 was used to develop an artificial base salts medium with similar chemistry to that present in sediment pore water for use in microcosm studies. The artificial pore water (PW) base salts medium consisted of NaF (6 μM), KCl (31 μM), $MgSO_4$ (86 μM), $CaSO_4$ (271 μM), $MgCO_3$ (5 μM), and $CaCO_3$ (22 μM). Nitrification microcosms consisted of 120-ml serum bottles containing 75 ml of pore water base salts medium amended with 1 mM NH_4Cl. Serum bottles were capped, sealed, sterilized by autoclaving, and cooled to 4°C. Sediments from RE (Fig. 1) were thawed at 4°C overnight prior to their use in microcosm studies. Cooled PW medium was inoculated aseptically with 7.5 g of wet weight subglacial sediment (6.1 g of dry weight). Following inoculation, bottles were capped and sealed. The gas phase was replaced by purging with filter-sterilized (0.22-μm pore size) air. Triplicate microcosms were incubated at both 4°C and 15°C. Killed controls were prepared by autoclaving serum bottles containing PW base salts medium and 7.5 g of subglacial sediment (25 min) and incubating the bottles at 4°C (24 h), followed by an additional round of autoclaving (25 min) and then incubation at 4°C and 15°C in the dark in parallel with the "live" experimental bottles. Approximately 2 ml of medium was removed every week via sterile syringe and needle for use in monitoring the concentration of NH_4^+, NO_2^-, and NO_3^-. Samples were centrifuged (14,000 × *g* for 2 min at 4°C) to remove particulate material and filter sterilized (0.2-μm-pore-size nylon filters) prior to analysis on a model MT-3 (SEALQuAAtro) segmented flow analyzer. The detection limit for these analytes is approximately 5 to 10 ppb. Serum bottles and their contents were kept at 4°C or 15°C during all manipulations.

Nitrate reduction potential assays. Nitrate reduction microcosms consisted of 120-ml serum bottles containing 75 ml of PW medium amended with 100 μM KNO_3. Prior to sterilization, the medium was purged with N_2 gas passed over heated copper shavings (210°C) for 30 to 45 min to remove any O_2. Bottles and PW medium were then capped, sealed, sterilized by autoclaving, and cooled to 4°C. Medium was inoculated with 7.5 g (wet weight) subglacial sediment (6.1 g of dry weight) by briefly removing the septa under a stream of sterile N_2 gas. Immediately after recapping, the headspace was degassed with filter-sterilized (0.22-μm pore size) N_2 gas. Killed controls were prepared as described above for the nitrification microcosms. The microcosms were incubated at 4°C, and samples were removed and processed for nitrogen species as described above. Serum bottles and their contents were kept at 4°C during all manipulations.

Nitrogen fixation potential assays. Microcosms for use in quantifying dinitrogen (N_2) fixation activity consisted of 25-ml serum bottles containing 4 ml of PW base salts medium. Prior to sterilization, the medium was purged for 30 to 45 min with N_2 gas passed over heated copper shavings (210°C). The serum bottles were then capped, sealed, and sterilized by autoclaving for 30 min. Serum bottles were chilled to 4°C, the bottles were uncapped, and 3.5 g of wet weight subglacial sediment (2.87 g of dry weight) was added to each bottle using an aseptic technique. While on ice, the bottles were recapped and sealed, and the headspace was again purged with filter-sterilized (0.22-μm pore size) N_2 gas for 25 min. Killed controls were prepared as described above for nitrification microcosms. Nitrogenase activity was assayed by the acetylene reduction technique (55). The nitrogenase assay was initiated by addition of 2.5 ml of 100% O_2-free acetylene into the headspace (final gas phase concentration of ~10% acetylene/90% nitrogen) using a presterilized gas-tight syringe. At various points during the incubation, the concentration of ethylene was determined in 50-μl subsamples of headspace gas sampled with a gas-tight syringe using a model GC-8A gas chromatograph (Shimadzu Corporation, Kyoto, Japan) equipped with an 80/100

Porapak Q (Supelco, St. Louis, MO) column and flame ionization detector. The injector temperature was held at 190°C, the column temperature was held at 120°C, and the carrier gas was helium. Triplicate biological controls, an uninoculated control, and a killed biological control were incubated at 4°C and 15°C. Serum bottles were kept at 4°C or 15°C during sampling.

N_2 fixation in snow-associated biomass sampled from the surface of the glacier (algal communities) was also examined. Four 500-ml bottles were packed with alga-containing surface snow during July 2008. The snow was collected from a location on the glacier surface that, when melted, would likely discharge into a crevasse in the glacier. Thus, ultimately the meltwater would be routed through the subglacial drainage system. Samples were frozen on-site using a dry ice-ethanol slurry and were kept at −20°C until processed. The samples were thawed at 4°C overnight, and the biomass from the melted snow was concentrated aseptically from a volume of ~250 ml to ~60 ml by centrifugation (5,000 × *g* for 5 min at 4°C). Microcosms consisted of sterilized 25-ml serum bottles containing 4 ml of concentrated surface snow biomass (~18 mg of dry solids). The bottles were capped and sealed using presterilized butyl rubber septa, wrapped in aluminum foil, and purged with filter-sterilized (0.22-μm pore size) N_2 for 25 min while keeping the serum bottles and contents at 4°C. Killed controls were prepared as described for the nitrification microcosms. A total of 2.5 ml of 100% acetylene was added to the headspace of each bottle (final gas phase concentration, 10% acetylene/90% nitrogen). Triplicate biological controls, an uninoculated control, and a killed biological control were incubated at 4°C and 15°C, and ethylene production was quantified as described above.

DNA extraction and functional gene analysis. Approximately 250 mg of wet weight sediment (~205 mg of dry weight) from each of the four samples collected in 2008 (two samples from each of the RE and RW sites) as well as two samples collected from RE and RW in 2009 were subjected to duplicate DNA extraction and purification as previously described (8). Equal volumes of each duplicate extract were pooled, and the DNA associated with the pooled volume was quantified fluorimetrically as previously described (8). The subglacial sediments collected contained approximately 22 ng of DNA per g of wet weight of sediment or approximately 30 ng of DNA per g of dry weight sediment (gdws). An approximately 450-bp fragment of the alpha subunit of the bacterial ammonia monooxygenase (*amoA*) gene was PCR amplified using primers amoA-1F (5′-GGGGTTTCTACTGGTGGT-3′) and amoA-2R (5′-CCCCTCKGSAAAGCCTTCTTC-3′) using an annealing temperature of 53°C (45). An approximately 635-bp fragment of the alpha subunit of the archaeal *amoA* gene was amplified using primers Arch-amoAF (5′-STAATGGTCTGGCTTAGACG-3) and Arch-amoAR (5′-GCGGCCATCCATCTGTATGT-3′) and an annealing temperature of 53°C (17). An approximately 650-bp fragment of the membrane-bound nitrate reductase (*narG*) gene was amplified using the primer pair narG-1960F (5′-TAYGTSGGCCARGARAA-3′) and narG-2659R (5′-TTYTCRTACCABGTBGC-3′) and an annealing temperature of 55°C (43). An approximately 400-bp fragment of the gene encoding the nitrogenase iron protein (*nifH*) was amplified using the primer pair nifH-119F (5′-THGTHGGYTGYGAYCCNAARGCNGAYTC-3′) and nifH-471R (5′-GGHGARATGATGGCNMTSTAYGCNGCNA A-3′) and a step-down PCR approach under the previously described conditions (20). Degenerate bases in all of the above primer sets are as follows: K represents G or T; S represents G or C; Y represents C or T; R represents A or G; B represents C, G, or T; H represents A, C, T; N represents A, C, T, or G; M represents A or C. For each primer pair (with the exception of *nifH*, as described in reference 20), ~1 ng of purified genomic DNA was subjected to PCR in triplicate using an initial denaturation at 94°C (4 min), followed by 35 cycles (bacterial *amoA*, *nifH*, and *narG*) or 40 cycles (archaeal *amoA*) of denaturation at 94°C (1 min), annealing at the specified temperature (1 min), primer extension at 72°C (1.5 min), and a final extension step at 72°C (20 min). The final reaction mixture (50 μl) contained 2 mM $MgCl_2$ (Invitrogen), 200 μM each deoxynucleotide triphosphate (Eppendorf, Hamburg, Germany), 0.5 μM each forward and reverse primer, 0.4 mg ml^{-1} molecular-grade bovine serum albumin (Roche, Indianapolis, IN), and 0.25 units of *Taq* DNA polymerase (Invitrogen) in 1× PCR buffer (Invitrogen). An equal volume of each replicate PCR amplification using DNA from RE (Fig. 1) sampled in July 2008 was pooled, purified, and subjected to sequence analysis according to previously described protocols (8).

Nucleotide sequences were translated in MEGA (version 4.0.1) (57), and the translated nucleotide sequences were aligned with the ClustalW application within MEGA specifying the Gonnet protein weight matrix with default gap extension and opening penalties. ClustalX (version 2.0.8) (31) was employed to generate pairwise sequence identity matrices for each aligned deduced amino acid sequence. Pairwise deduced amino acid sequence identity matrices were used to determine the number of unique phylotypes using DOTUR (46) with the nearest neighbor algorithm and a precision of 0.01. DOTUR was also used to estimate Simpson's index of diversity (100% sequence identities), where values of 1 indicate infinite diversity and values of 0 indicate no diversity.

qPCR. Quantitative PCR (qPCR) was used to estimate the number of archaeal and bacterial *amoA* templates, the number of *narG* templates, and the number of *nifH* templates associated with RE sediments sampled in 2008. Quantitative PCR generally followed the method of Mosier and Francis (38). In brief, archaeal *amoA* and bacterial *amoA*, *narG*, and *nifH* were PCR amplified from plasmid clones specific for each gene (see Table S1 in the supplemental material) using 30 cycles of PCR as described above. The PCR products were purified and quantified fluorimetrically as described above for use in generating standard curves. Standard curves relating template copy number to threshold qPCR amplification signal were constructed for each target gene by using dilutions of two plasmid clones. The abundances of functional genes derived using standard curves generated from the two functional gene phylotypes for each target gene were similar (varied by no more than a factor of 1.5) and thus were averaged for use in calculating the average and standard deviation of template abundances from replicate qPCRs. For AOA *amoA* quantification, a standard curve was generated over 5 orders of magnitude from 8.6×10^2 to 8.6×10^7 copies of template per assay ($R^2 = 0.987$), whereas for AOB *amoA* quantification, a standard curve was generated over 5 orders of magnitude from 6.2×10^2 to 6.2×10^7 copies of template per assay ($R^2 = 0.998$). For *nifH*, a standard curve was generated over 5 orders of magnitude from 0.9×10^1 to 1.1×10^6 ($R^2 = 0.997$) copies of template per assay, whereas a standard curve for *narG* was generated over 4 orders of magnitude from 0.6×10^1 to 2.6×10^5 copies of template per assay ($R^2 = 0.992$). The detection limit for AOA and AOB *amoA* was ~20 copies of template per assay, and for *nifH* and *narG* it was ~5 to 10 copies per assay. qPCRs were performed in 0.5-ml optically clear PCR tubes (Corbett, Sydney, Australia) in a Rotor-Gene 3000 quantitative real-time PCR machine (Corbett) using an SsoFastTM EvaGreen Supermix (Bio-Rad Laboratories, Hercules, CA). The following cycling conditions were utilized for *amoA* reactions: initial denaturation (95°C for 4 min), followed by 40 cycles of denaturation (95°C for 45 s), annealing (at 53°C for bacterial and archaeal *amoA*], 55°C for *narG*, and 60.9°C for *nifH* for 60 s), and extension (72°C for 60 s). Product specificity was verified by melt curve analysis. The template abundances reported reflect the average and standard deviation of three replicate qPCR analyses for each functional gene.

Nucleotide sequence accession numbers. Nucleotide sequences have been deposited in the GenBank, DDBJ, and EMBL databases under accession numbers HQ650066 to HQ650079 (archaeal *amoA*), HQ650005 to HQ650022 (bacterial *amoA*), HQ650023 to HQ650065 (*narG*), and HQ650080 to HQ650083 (*nifH*) (see Tables S1 and S2 in the supplemental material).

RESULTS

Subglacial bulk meltwater and sediment pore water chemistry. Saturated subglacial sediments were sampled in July 2008 from RE for use in determining sediment pore water chemistry. Ammonium (2.5 μM), nitrite (0.3 μM), and nitrate (3.9 μM) were detected in sediment pore water (Table 1), suggesting that the sediment-associated communities may be actively cycling N compounds and/or that the sediments are N limited, possibly due to microbial activity. Differences in solute concentrations between sediment pore waters and bulk subglacial meltwaters can provide insight into nutrient sources and sinks in the subglacial environment. While the dissolved organic carbon (DOC) in RE sediment pore waters (60.0 μM C) was a factor of 3 greater that the DOC in RE subglacial bulk meltwaters (18.3 μM C), the dissolved organic nitrogen (DON) in RE sediment pore waters (0.3 μM N) was a factor of 5.5 lower than the DON in the RE bulk meltwaters (1.6 μM N) (Table 1). This observation suggests that the dissolved organic C is recalcitrant to microbial utilization or may indicate the preferential utilization of organic N relative to organic C in the dissolved organic fraction in sediment pore waters.

The concentrations of NO_3^-, NO_2^-, and NH_4^+ (similar to those of the other ions) were notably lower in samples of RE bulk subglacial meltwaters sampled in July 2008 than in the RE

TABLE 1. Geochemical and physical characteristics of subglacial sediment pore water and subglacial bulk meltwater[a]

Sample (collection date)	Physical and chemical profile						Cation concn (μM)					Anion concn (μM)[c]					
	T (°C)	pH	EC (μS/cm)	DO (mg/liter)	DOC (μM/liter)[b]	DON (μM/liter)	DOC/DON	NH_4^+	Na^+	K^+	Mg^{2+}	Ca^{2+}	Mo^{2+}	NO_3^-	NO_2^-	PO_4^{3-}	Cl^-	SO_4^{2-}	HCO_3^-
RE pore water (July 2008)	NA	NA	NA	NA	60.0	0.3	210	2.5 (0.1)	5.9	30.6	171.5	449.2	0.052	3.9 (0.1)	0.3 (<0.1)	0.04 (<0.01)	3.4	270.8	913
RE meltwater (July 2008)	1.0	6.7	15.9	NA	18.3 (1.7)	1.6 (1.4)	12	0.9 (0.01)	0.3 (0.03)	0.2 (0.03)	7.3 (1.5)	91.6 (5.8)	NA	2.4 (0.2)	BD[d]	NA	0.1 (0.03)	2.2 (0.3)	176
RW meltwater (July 2008)	0.6	7.6	49.9	NA	30.8 (1.7)	5.1 (1.4)	6	0.9 (0.01)	1.2 (0.03)	0.9 (0.03)	41.5 (1.5)	247.2 (5.8)	NA	3.2 (0.2)	BD[d]	NA	0.3 (0.03)	39.7 (0.3)	498
RE meltwater (September 2009)	0.3	8.8	32.5	11.3	33.3	NA	NA	BD[d]	NA	NA	39.9 (0.5)	277.0 (4.2)	BD[d]	2.0 (0.3)	BD[d]	0.19 (0.02)	5.5 (0.2)	75.1 (0.7)	330
RW meltwater (September 2009)	0.1	8.7	32.0	10.9	24.2	NA	NA	BD[d]	NA	NA	33.4 (0.4)	264.5 (2.9)	BD[d]	3.0 (0.1)	BD[d]	0.11 (0.01)	1.5 (0.1)	33.1 (0.1)	413

[a] Standard errors for replicate analyses are indicated in parentheses, where available. Abbreviations: NA, not available; BD, below detection; T, temperature; EC, electrical conductivity; DOC, dissolved organic carbon; DON, dissolved organic nitrogen; DO, dissolved oxygen.
[b] Sediment pore water was assayed as nonpurgeable organic carbon. Subglacial meltwaters were assayed as DOC.
[c] Sediment pore water was assayed as phosphate ions. Subglacial meltwaters were assayed as total P.
[d] Detection limits were as follows: Mo^{2+}, 1 nM; NO_2^-, 25 nM.

sediment pore water also sampled in 2008 (Table 1), suggesting that the sediments may be a source for these analytes in the subglacial meltwaters. In contrast, DON was higher in the RE bulk subglacial meltwater than in the pore waters. Concentrations of inorganic solutes, as well as organic C and N, were generally higher in bulk subglacial meltwaters sampled from RW than RE during July 2008, which likely reflects differences in the subglacial hydrological flow paths that control water/rock ratios and contact times, which lead to differences in solute acquisition.

The concentration of dissolved inorganic N species in bulk meltwaters in all four samples collected in July 2008 and September 2009 were either similarly low (for 2008 samples, NO_3^- and NH_4^+) or were below detection (2009 samples, NO_2^- and NH_4^+) (Table 1). The differences in other RW ion concentrations between samples collected in July 2008 and September 2009 were minor, whereas increases in ion concentrations were noted in the RE samples collected in September 2009 compared to those collected in July 2008. This was especially true for the cations Mg^{2+} and Ca^{2+} and the anions Cl^-, SO_4^{2-}, and HCO_3^- (Table 1). A significant (2 pH units) increase in pH was also noted between measurements made in 2008 and 2009. This difference may reflect a change to a less efficient hydrological flow path in the RE subglacial drainage system, leading to increased residence times which, in turn, could increase water-rock interactions and alter solute composition (58).

Functional gene richness, phylogenetic diversity, and template abundance. Four different subglacial sediment samples (two from RE and two from RW) collected in July 2008 and two different subglacial sediment samples (one from RE and one from RW) collected in September 2009 were screened for biomarker genes indicative of the potential for nitrification (ammonia monoxygenase subunit A [*amoA* gene]), nitrogen fixation (nitrogenase iron protein [*nifH* gene]), and nitrate reduction (dissimilatory nitrate reductase [*narG* gene]) using PCR. Fragments of the predicted sizes were detected by PCR for each gene with template DNA extracted from all six sediment samples. This suggests the potential for these processes to occur in subglacial sediments at multiple locations close to the glacier terminus on an interannual basis. Bacterial and archaeal *amoA*, *narG*, and *nifH* gene amplicons obtained from RE in July 2008 were selected for further sequence and qPCR analysis since corresponding sediment pore water and bulk meltwater chemistry was available for this sample, with the following results.

(i) Archaeal ammonia monooxygenase subunit A (*amoA*). The abundance of ammonia-oxidizing archaeal (AOA) *amoA* genes in RE sediments was below the detection limit of our qPCR assay, indicating that nitrifying archaea are likely to be a minor component of the subglacial microbial community (<20 *amoA* gene copies per $gdws^{-1}$). However, we were still able to amplify the gene from the sediments using 40 cycles of traditional PCR, and after pooling and purifying three replicate PCRs, we were able to generate a high enough concentration of *amoA* amplicons to clone and sequence. Of the total 44 AOA *amoA* inferred protein sequences recovered, 14 were unique, resulting in a predicted Simpson diversity index of 0.67. The majority of AOA AmoA sequences exhibited close affiliation (98 to 100% sequence identities) with clones previously recovered from the sediments and water column at sev-

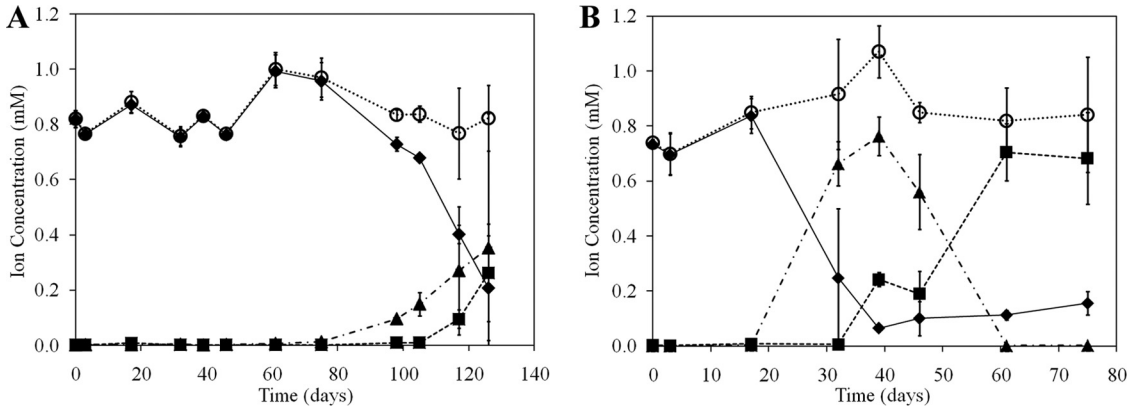

FIG. 2. Concentrations of NH_4^+ (◆), NO_2^- (▲), NO_3^- (■), and total soluble N (○) as a function of time in microcosms incubated at 4°C (A) and 15°C (B) with 1 mM NH_4^+ added. Total soluble N is the sum of the concentrations of NH_4^+, NO_2^-, and NO_3-. Values represent the difference in concentrations between biological replicates and killed controls. The standard deviation of three replicates is indicated.

eral sites in the San Francisco North Bay estuary (see Table S1 in the supplemental material). Among cultivated isolates, the AOA AmoA sequences were 95 to 96% identical to the AmoA sequence from *Nitrosopumilus maritimus* SCM1 (see Table S2), a marine chemolithotrophic nitrifier (30). It is unclear what physicochemical parameters in the RG subglacial environment would select for nitrifying organisms similar to this marine strain, considering that the RG subglacial meltwaters exhibit conductivities ranging from 15 to 50 $\mu S\ cm^{-1}$ (Table 1), which are typical of freshwater environments.

(ii) Bacterial ammonia monooxygenase subunit A (*amoA*). Ammonia-oxidizing bacterial (AOB) *amoA* genes were detected in the RE sediment sample at an abundance of 1,602 ± 62 copies $gdws^{-1}$. The bacterial *amoA* genes recovered from RE subglacial sediment were considerably more diverse than the archaeal *amoA* genes sampled from the same site. Of the 36 AOB *amoA* inferred protein sequences obtained, 18 were unique, resulting in a predicted Simpson diversity index of 0.94. Roughly 35% of the bacterial AmoA sequences exhibited close affiliations with environmental clones recovered from sediments sampled from the San Francisco Bay estuary, with another 32% exhibiting affiliation with sequences from freshwater sediment environments (see Table S1 in the supplemental material). The remaining 33% of the AOB AmoA sequences exhibited affiliation with clones obtained from terrestrial soils. Among cultivated organisms, the AOB AmoA sequences were most closely affiliated (>90% sequence identities) to AmoA from organisms within the betaproteobacterial order *Nitrosomonadales* (see Table S2).

(iii) Dissimilatory nitrate reductase subunit G (*narG*). NarG-encoding genes were detected in RG sediments at an abundance of 662 ± 49 copies $gdws^{-1}$. Of the 49 *narG* inferred protein sequences obtained, 43 were unique, resulting in a predicted Simpson's diversity index of 0.98. The RE subglacial sediment-associated NarG sequences differed from each other by up to 59% sequence identity (average sequence identity is 63.2%). Compared to environmental clones, the majority of the RG NarG sequence phylotypes were most similar (70 to 95% sequence identities) to sequences recovered from sediment environments and from invertebrate gut environments (see Table S1 in the supplemental material). Intriguingly, two of the NarG phylotypes were similar (93% sequence identities) to environmental clones recovered from a soil developed on the forefield of a retreating Alpine glacier (13). All of the NarG sequences were generally distantly related to NarG from cultivated bacteria, as indicated by the average percent identity of 84% (see Table S1). The majority (47%) of RG NarG sequences were most closely affiliated (75 to 96% sequence identities) with NarG from *Polaromonas* spp., a genus within the betaproteobacterial order *Burkholderiales* (see Table S2), with cold-tolerant members isolated from Arctic and Antarctic environments (25, 49). The remaining RG NarG sequences exhibited close relation to *Gamma-* and *Deltaproteobacteria*, as well as *Actinobacteria*.

(iv) Nitrogenase iron protein (*nifH*). NifH-encoding genes were detected in RG at an abundance of 311 ± 23 copies $gdws^{-1}$. A total of 11 *nifH* inferred protein sequences were obtained from the RE subglacial sediments, of which four were unique, resulting in a predicted Simpson diversity index of 0.60. Interestingly, the RG NifH sequences were most closely related to NifH sequences recovered from geothermal springs in Yellowstone National Park, Wyoming (see Table S1 in the supplemental material). Compared to *nifH* inferred protein sequences from cultivated organisms, 10 of the 11 sequences were most closely affiliated (94 to 95% sequence identities) with NifH from *Methylocella silvestris* (see Table S2), a mesophilic alphaproteobacterium within the order *Rhizobiales*.

Potential inorganic nitrogen compound transformation rates. (i) Potential nitrification rates. Potential nitrification rates were determined in microcosms containing subglacial sediments in artificial pore water with minimal nutrient amendment. Ammonium was added to each sample to initiate the microcosm experiment, and NH_4^+, NO_2^-, and NO_3^- concentrations were monitored in microcosms incubated at both 4°C and 15°C (Fig. 2A and B, respectively). A significant ($P = 0.05$) decrease in NH_4^+ concentration and a stoichiometric and significant ($P < 0.01$) increase in NO_2^- concentration was observed over the period of 17 to 39 days of incubation at 15°C. Over this duration, the rate of NH_4^+ removal was 0.43 ± 0.05 $\mu mol\ N\ gdws^{-1}\ day^{-1}$, and the rate of NO_2^- production was 0.42 ± 0.06 $\mu mol\ N\ gdws^{-1}\ day^{-1}$. Assuming that the ammonia oxidation activity associated with microcosms is attribut-

able to AOB (AOA *amoA* genes were at least 3 orders of magnitude less abundant than AOB *amoA*), that AOB in RE sediments encode 2.5 copies of *amoA* per genome on average (40), and that AOB are not growing (AOB template abundance did not change during course of incubation [data not shown]), the maximum potential rate of ammonia oxidation in RE sediments observed over the 17- and 39-day incubation time was 28.1 pmol of NH_4^+ oxidized per cell h^{-1}. At 39 days of incubation, oxidation of NH_4^+ had ceased, and oxidation of NO_2^- to NO_3^- had commenced, as indicated by a significant ($P < 0.01$) increase in NO_3^- concentration and the NO_2^- concentration reaching a plateau. At 61 days of incubation, the oxidation of NO_2^- appeared to terminate, with roughly 90% of the added NH_4^+ converted to NO_2^- and ultimately NO_3^- over this period.

Ammonia oxidation in microcosms incubated at 4°C commenced between 75 and 98 days, as indicated by a significant ($P = 0.02$) decrease in NH_4^+ concentration and a near stoichiometric and significant ($P < 0.01$) increase in NO_2^- concentration (Fig. 2A). Maximal nitrification activity was observed during the period spanning 105 and 117 days of incubation, with a NH_4^+ oxidation rate of 0.28 ± 0.04 μmol N $gdws^{-1}$ day^{-1} and a NO_2^- production rate of 0.12 ± 0.19 μmol N $gdws^{-1}$ day^{-1}. Assuming that the ammonia oxidation activity associated with microcosms is attributable to AOB and that AOB encode 2.5 copies of *amoA* per genome on average (40), the maximum potential rate of ammonia oxidation in RE sediments observed between days 105 and 117 was 10.1 pmol of NH_4^+ oxidized per cell h^{-1}. A significant increase ($P = 0.01$) in NO_3^- concentration was observed at 117 days compared to the concentration at 105 days. A comparison of the maximal rate of nitrification, as measured by NH_4^+ oxidation, revealed a statistically insignificant difference ($P = 0.25$) between microcosms incubated at 4°C or 15°C. Thus, the primary difference in nitrification in microcosms incubated at 4°C and 15°C was in the lag phase, which was approximately three times shorter at 15°C than at 4°C.

(ii) Potential nitrate reduction rates. Potential nitrate reduction rates were determined in microcosms containing subglacial sediments in artificial pore water with minimal nutrient amendment. Nitrate was added to each sample to initiate the microcosm experiment, and the concentrations of NH_4^+, NO_3^-, and NO_2^- were monitored in microcosms incubated at 4°C only since previous experiments showed nitrate utilization in subglacial sediments sampled from a polythermal glacier with broadly similar physicochemical properties when they were incubated in the presence of NO_3^- at 4°C (51). A significant ($P = 0.02$) decrease in NO_3^- concentration and a significant ($P = 0.04$) and stoichiometric increase in NO_2^- were observed over the incubation period spanning 33 to 43 days when incubation was at 4°C (Fig. 3). Over this duration, the rate of NO_3^- removal was 18.5 ± 8.1 nmol of N $gdws^{-1}$ day^{-1}, and the rate of NO_2^- production was 19.1 ± 1.0 nmol of N $gdws^{-1}$ day^{-1}, indicating that the NO_3^- was being converted to NO_2^- and was not being assimilated. Importantly, no increase in NH_4^+ concentration was noted during the incubation period, and no change in soluble inorganic N was noted, indicating that the further oxidation of NO_2^- to a gaseous substrate (NO, N_2O, and N_2) during denitrification or that production of NH_4^+ from NO_2^- during ammonification had yet to commence, assuming that organisms in the sediment community have the capacity to perform such reactions at 4°C. Unfortunately, we could not determine if either of these two processes was occurring in the RE sediments since frequent sampling during the early stages of the incubation precluded additional sampling beyond 55 days.

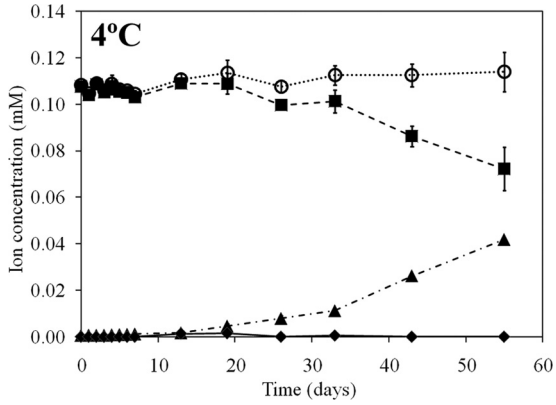

FIG. 3. Concentrations of NH_4^+ (◆), NO_2^- (▲), NO_3^- (■), and total soluble N (○) as a function of time in microcosms incubated at 4°C with 100 μM NO_3^- added. Total soluble N is the sum of the concentrations of NH_4^+, NO_2^-, and NO_3^-. Values represent the difference in concentrations between biological replicates and killed controls. The standard deviation of three replicates is indicated (error bars in NH_4^+ and NO_2^- are smaller than symbol size).

(iii) Potential nitrogen fixation rates. The potential for nitrogen fixation in microbial communities associated with subglacial sediments and surface snow algal communities was assessed using the acetylene reduction technique. Even when microcosms were incubated for 240 days at 4°C and 15°C, ethylene was not observed to accumulate in the headspace of either set of microcosms (data not shown).

DISCUSSION

The presence of populations capable of nitrification and nitrate reduction in subglacial environments was initially suggested by *ex situ* microcosm experiments (16, 51) and nutrient budgets derived from geochemical and isotopic studies (21, 23, 62). Elevated organic C/N ratios in sediments sampled from beneath RG (9) also suggested the potential for recent microbial depletion of N in the organic matter, presumably through mineralization followed by nitrification and denitrification although further analysis of subglacial sediments is required to confirm this. The detection of both archaeal and bacterial *amoA*, *narG*, and *nifH* genes in sediments sampled from RE and RW in both July 2008 and September 2009 provides the first genetic evidence in support of a role for microorganisms in the subglacial nitrogen cycle.

Bacterial AmoA was found to be more diverse than archaeal AmoA in sediments sampled from RG, a finding that is consistent with the >3 orders of magnitude higher abundance of bacterial *amoA* templates than archaeal *amoA* templates in the subglacial sediments. The detection of *amoA* genes affiliated with archaea in RG sediments as reported here is only the second account of archaea in a subglacial environment (9) and is the first report of genes affiliated with *Thaumarchaeota* re-

covered from such systems. However, the dominance of AOB over AOA was not anticipated in the RG sediments in light of a number of recent studies suggesting that archaea often predominate among nitrifiers in soil/sediment environments with similar physical and chemical characteristics to that of RG sediments (3, 32, 63, 65). While a number of factors have been hypothesized to influence the relative abundance of AOA relative to AOB in natural environmental systems (3, 34, 38, 39), the global controls on these two populations remain ambiguous, and it seems unlikely that the parameters that have been suggested to constrain the abundance of AOA and AOB in other environments are necessarily responsible for their observed abundances in RG. For example, AOA have been shown to predominate over AOB in fresh to slightly brackish estuarine sediments with elevated sediment organic C/N ratios of >12 (38). However, in the freshwater RG sediments which have a sediment organic C/N ratio of ~137 (9), AOB predominate. Likewise, AOA were shown to be better adapted than AOB for growth under conditions of nutrient stress, including conditions where ammonia concentrations are extremely low (34). However, in the freshwater RG sediments that have low bulk meltwater and pore water ammonium concentrations, AOB predominate. The ratio of AOA to AOB *amoA* genes and gene transcripts in soils has been shown to be sensitive to pH, with the shift from AOA-dominated communities to AOB-dominated communities occurring at a slightly acidic pH of 6.5 (39). The circumneutral pH associated with samples collected in July and the shift to more alkaline pH in meltwaters sampled in September may select for bacterial nitrifiers over archaeal nitrifiers. Additional analyses of subglacial sediment pore water geochemistry in relation to AOA and AOB *amoA* gene abundances in glacial systems with differing physico-chemical properties (e.g., glaciers underlain by different bedrock) and sampled over a seasonal hydrological cycle will be required to elucidate the most influential controls on AOA and AOB assemblages in subglacial ecosystems.

The maximum rate of ammonia oxidation in microcosms incubated at 4°C was ~50% lower than the maximum rate observed in microcosms incubated at 15°C, a finding that is consistent with a number of studies that indicate a positive relationship between nitrification rate and temperature (5, 18, 33). The mean potential nitrification rates determined for RE sediments (28.1 and 10.1 pmol of NH_3 oxidized per cell h^{-1} at 15°C and 4°C, respectively) were elevated relative to rates determined for a number of agricultural soils incubated at 25°C (0.20 to 13.5 fmol of NH_3 oxidized per cell h^{-1}) (26, 41) and to those determined for sediments sampled from the San Francisco Bay estuary incubated at 22°C ($1.6 \times 10^{-2} \pm 0.7 \times 10^{-2}$ to $2.9 \times 10^{-4} \pm 0.6 \times 10^{-4}$ fmol of NH_3 $cell^{-1}$ h^{-1}) (4). The differences in potential activities associated with these studies may reflect differences in the physiological state of the cells that were assayed and may be attributable to the influence of NH_4^+ amendment during incubation. This follows from the fact that evidence of nitrification was apparent following 1 to 3 days of incubation in microcosms containing sediment from the San Francisco Bay when they were incubated at 22°C (4) and was apparent following 7 days incubation in microcosms containing agricultural soils incubated at 25°C (26), whereas evidence for nitrification was not apparent in RG microcosms until 17 and 105 days of incubation when they were incubated at 15°C and 4°C, respectively. The longer lag time observed in the present study is unlikely to be due to growth of nitrifiers during incubation since microcosms contained minimal nutrient amendment and since qPCR analyses of *amoA* abundances in sediments from microcosms sampled at the end of the experiment did not indicate a significant increase in *amoA* gene copy number for AOA or AOB compared to sediments sampled at the start of the incubations (data not shown). Rather, the long lag times in substrate utilization observed in RG microcosms may reflect lower basal levels of nitrification activity *in situ* and/or may reflect *amo* induction and *de novo* protein synthesis in response to the added ammonium. This possibility is supported by the observed low ammonium concentrations in sediment pore water and meltwaters at RG (<2.5 μM), which are generally below the minimum ammonium threshold concentration (~10 μM) shown to be metabolized in cultures of the cultivated nitrifying bacteria (7). Thus, the actual *in situ* rate of nitrification in the RG subglacial environment is likely to be lower than that reported here.

A diversity of *narG* genes was also detected in subglacial sediments from RG, with 7 of the 43 unique NarG phylotypes identified in RG subglacial sediments exhibiting close affiliation (~95% sequence identities) with NarG clones recovered from the forefield of the geographically distinct Rotmoosferner Glacier, Austria (13). This may indicate that the physicochemical properties of glaciated environments select for unique lineages of nitrate-reducing bacteria. The maximal rate of nitrate reduction observed in RG microcosms incubated at 4°C (18.5 nmol of N $gdws^{-1}$ day^{-1} or 22.1 nmol of N gram $sediment^{-1}$ day^{-1}) is similar to that reported for coastal marine sediments at an *in situ* temperature of 2.5°C (35 nmol of N gram $sediment^{-1}$ day^{-1}) (53) and is comparable to rates determined for recently deglaciated soils from Rotmoosferner Glacier incubated at 25°C (7 nmol of N $gdws^{-1}$ day^{-1}; value derived by dividing 25-yr rhizosphere soil nitrate reduction rate by a factor of 23, as reported in Deiglmayr et al. [13]). If it is assumed that two copies of *narG* exist per genome (42) and that ~50% of nitrate reduction activity observed in an environment is attributable to Nar, with the remainder attributable to Nap (based on similar abundances of *narG* and *napA* in a variety of environments [10]), the per cell normalized nitrate reduction potentials observed in RE subglacial sediments incubated at 4°C (580 fmol of NO_3^- reduced $cell^{-1}$ h^{-1}) were within an order of magnitude of those observed in estuarine sediments incubated at 15°C (48 to 326 fmol of NO_3^- reduced $cell^{-1}$ h^{-1}) (14). Like nitrification assays with RG sediment, there was a significant lag time (33 days) in RG microcosms prior to any measurable nitrate reduction. This lag phase is similar to the lag phase of ~18 days reported in 4°C incubations of melted basal ice (ice containing significant subglacial sediment) from John Evans Glacier, Canada (51). Both of these extended lag phases likely point to lower basal levels of nitrate reduction activity *in situ*. Thus, as with the potential nitrification rates, the potential nitrate reduction rates reported here likely reflect the upper limit of *in situ* rates.

The subglacial sediments at RG are depleted in N, as indicated by elevated C/N atomic ratios of ~137 in particulate organic matter in the sediment (9) and by low overall concentrations of fixed N in pore waters and in the bulk meltwaters. However, concentrations of bulk meltwater nutrients, includ-

ing nitrate and ammonium, are known to vary by ~5- to 15-fold during a seasonal hydrologic cycle at RG (M. Lafrenière, unpublished data), which may result in seasonal differences in N availability and N cycling processes in the subglacial environment. The dissolved organic matter in sediment pore waters reveals elevated C/N atomic ratios of ~210, which were an order of magnitude higher than the C/N atomic ratios of 6 to 12 in bulk subglacial meltwaters (Table 1). This observation may reflect the preferential utilization of N relative to C by sediment-associated microbial populations (27). The C/N ratios in sediment organic matter and in sediment pore water organic matter, in the context of low dissolved inorganic and organic N concentrations in subglacial sediment pore water and bulk meltwater, indicate that these environments are N limited. Biological nitrogen fixation is of fundamental importance in natural ecosystems since it can relieve fixed N limitation (64). Despite the presence of ~300 *nifH* gene copies $gdws^{-1}$, we were unable to detect N_2 fixation activity in subglacial sediments even after 240 days of incubation. The inability to fix N_2 biologically in the sediments would presumably render them as a sink for fixed nitrogen. This implies that NH_4^+ in subglacial environments is unlikely to be the result of localized biological N_2 fixation and, instead, results from mineral weathering sources (e.g., shales [22]) and/or surficial input.

Despite the detection of *nifH* genes in DNA extracted from a supraglacial red snow algal community sampled from above a series of crevasses where supraglacial waters enter the subglacial hydrological network, attempts to detect N_2 fixation in this biomass were unsuccessful. This finding is consistent with very low surficial inputs of NH_4^+, which are always less than 0.9 μM and usually below detection (<0.2 μM) in supraglacial meltwaters sampled in the summers of 2006, 2007, and 2008 (Lafrenière, unpublished). The lack of detectable N_2 fixation activity and the temporal variability in NH_4^+ in RG supraglacial meltwaters may implicate an important role for exogenous sources of fixed nitrogen at RG. Large NO_3^- and NH_4^+ depositional events have been documented at high-latitude glaciers in Svalbard (21), where these events were hypothesized to be an important source of N to the glacial system. Stibal et al (56), working on a different Svalbard glacier, argue that the majority of organic carbon on the glacier surface, and thus a potential source for the subglacial system through crevasses and moulins, is allochthonous wind-blown debris. Such allochthonous organic carbon is also likely to contain significant organic N, which would then be available for mineralization with subsequent nitrification and denitrification.

In summary, the results presented here indicate the presence of a diversity of microorganisms that are likely to be supported through the redox transformation of inorganic nitrogen compounds and possibly organic nitrogen compounds. Potential rates of nitrification and nitrate reduction were similar to those measured in other cold environments such as marine sediments, suggesting that these processes in subglacial environments may be an important and previously overlooked component of the global N cycle. It is important to note that the rates determined here for RG subglacial sediments likely reflect the upper limit of *in situ* rates; further efforts are needed to bridge the gap between potential rates determined in laboratory microcosms and *in situ* rates. Previous studies have shown that coupled nitrification and denitrification in marine systems contribute the greenhouse gases NO and N_2O to the atmosphere and thereby have the potential to influence biogeochemical cycles on glacial-interglacial timescales (1). N_2O production in subglacial systems is also consistent with reports of elevated concentrations of N_2O in basal ice layers of a tropical ice core (11). This finding was interpreted as indicating microbial N_2O production *in situ* at subzero temperatures, as later demonstrated in the laboratory using the AOB *Nitrosomonas cryotolerans* (37). While *amoA* sequences affiliated with *N. cryotolerans* were not recovered from RG subglacial sediments, sequences affiliated with *Nitrosomonas aestuarii* were, suggesting that an organism similar to *N. aestuarii* may contribute N_2O to the subglacial environment. Considering that ice currently covers 11% of the terrestrial landmass and that it covered a significantly greater portion of Earth at times in the past (29), the potential for nitrification and nitrate reduction in subglacial environments as demonstrated here furthers our understanding of the potential for these environments to contribute to global biogeochemical cycles on glacial-interglacial timescales.

ACKNOWLEDGMENTS

This research was supported by NASA Exobiology Grant NNX10AT31G (E.S.B., J.W.P., and M.S.), a grant from the Montana Space Grant Consortium (E.S.B. and A.C.M.), and NSERC Discovery Grant 311928 (M.J.L.). The Astrobiology Biogeocatalysis Research Center was supported by NASA Astrobiology Institute (NAI) grant NNA08C-N85A (E.S.B. and J.W.P.). E.S.B. was supported by an NAI postdoctoral fellowship, T.L.H. was supported by an NSF Integrated Graduate Educational Research and Training fellowship grant (NSF DGE 0654336), and R.K.L. acknowledges support from the Montana State University Undergraduate Scholars Program.

We thank the staff at the Biogeosciences Institute at the University of Calgary's Kananaskis Field Station for use of field and laboratory facilities.

REFERENCES

1. **Algeo, T., et al.** 2008. Changes in ocean denitrification during Late Carboniferous glacial-interglacial cycles. Nat. Geosci. **1:**709–714.
2. **Beaumont, V., and F. Robert.** 1999. Nitrogen isotope ratios of kerogens in Precambrian cherts: a record of the evolution of atmospheric chemistry? Precambrian Res. **96:**63–82.
3. **Bernhard, A. E., et al.** 2010. Abundance of ammonia-oxidizing *Archaea* and *Bacteria* along an estuarine salinity gradient in relation to potential nitrification rates. Appl. Environ. Microbiol. **76:**1285–1289.
4. **Bernhard, A. E., J. Tucker, A. E. Giblin, and D. A. Stahl.** 2007. Functionally distinct communities of ammonia oxidizing bacteria along an estuarine salinity gradient. Environ. Microbiol. **9:**1439–1447.
5. **Berounsky, V. M., and S. W. Nixon.** 1993. Rates of nitrification along an estuarine gradient in Narragansett Bay. Estuaries **16:**718–730.
6. **Bhatia, M., M. J. Sharp, and J. Foght.** 2006. Distinct bacterial communities exist beneath a high arctic polythermal glacier. Appl. Environ. Microbiol. **72:**5838–5845.
7. **Bollmann, A., M.-J. Bar-Gilissen, and H. J. Laanbroek.** 2002. Growth at low ammonium concentrations and starvation response as potential factors involved in niche differentiation among ammonia-oxidizing bacteria. Appl. Environ. Microbiol. **68:**4751–4757.
8. **Boyd, E. S., et al.** 2007. Isolation, characterization, and ecology of sulfur-respiring *Crenarchaea* inhabiting acid-sulfate-chloride geothermal springs in Yellowstone National Park. Appl. Environ. Microbiol. **73:**6669–6677.
9. **Boyd, E. S., M. Skidmore, A. C. Mitchell, C. Bakermans, and J. W. Peters.** 2010. Methanogenesis in subglacial sediments. Environ. Microbiol. Rep. **2:**685–692.
10. **Bru, D., A. Sarr, and L. Philippot.** 2007. Relative abundances of proteobacterial membrane-bound and periplasmic nitrate reductases in selected environments. Appl. Environ. Microbiol. **73:**5971–5974.
11. **Campen, R. K., T. Sowers, and R. B. Alley.** 2003. Evidence of microbial consortia metabolizing within a low-latitude mountain glacier. Geology **31:** 231–234.
12. **Cheng, S. M., and J. M. Foght.** 2007. Cultivation-independent and -dependent characterization of bacteria resident beneath John Evans Glacier. FEMS Microbiol. Ecol. **59:**318–330.

13. **Deiglmayr, K., L. Philippot, D. Tscherko, and E. Kandeler.** 2006. Microbial succession of nitrate-reducing bacteria in the rhizosphere of *Poa alpina* across a glacier foreland in the Central Alps. Environ. Microbiol. **8:**1600–1612.
14. **Dong, L. F., et al.** 2009. Changes in benthic denitrification, nitrate ammonification, and anammox process rates and nitrate and nitrite reductase gene abundances along an estuarine nutrient gradient (the Colne Estuary, United Kingdom). Appl. Environ. Microbiol. **75:**3171–3179.
15. **Flanagan, D. A., et al.** 1999. Detection of genes for periplasmic nitrate reductase in nitrate respiring bacteria and in community DNA. FEMS Microbiol. Lett. **177:**263–270.
16. **Foght, J., et al.** 2004. Culturable bacteria in subglacial sediments and ice from two southern hemisphere glaciers. Microb. Ecol. **47:**329–340.
17. **Francis, C. A., K. J. Roberts, J. M. Beman, A. E. Santoro, and B. B. Oakley.** 2005. Ubiquity and diversity of ammonia-oxidizing archaea in water columns and sediments of the ocean. Proc. Natl. Acad. Sci. U. S. A. **102:**14683–14688.
18. **Frederick, L. R.** 1956. The formation of nitrate from ammonium nitrogen in soils: I. Effect of temperature. Soil Sci. Soc. Am. J. **20:**496–500.
19. **Garvin, J., R. Buick, A. D. Anbar, G. L. Arnold, and A. J. Kaufman.** 2009. Isotopic evidence for an aerobic nitrogen cycle in the latest Archean. Science **323:**1045–1048.
20. **Hamilton, T. L., E. S. Boyd, and J. W. Peters.** 2011. Environmental constraints underpin the distribution and phylogenetic diversity of *nifH* in the Yellowstone geothermal complex. Microb. Ecol. **61:**860–870.
21. **Hodson, A., T. J. Roberts, A.-C. Engvall, K. Holmén, and P. Mumford.** 2010. Glacier ecosystem response to episodic nitrogen enrichment in Svalbard, European High Arctic. Biogeochemistry **98:**171–184.
22. **Holloway, J. M., and R. A. Dahlgren.** 2002. Nitrogen in rock: Occurrences and biogeochemical implications. Global Biogeochem. Cycles **16:**1118.
23. **Hopmans, E. C., et al.** 2004. A novel proxy for terrestrial organic matter in sediments based on branched and isoprenoid tetraether lipids. Earth. Planet. Sci. Lett. **224:**107–116.
24. **Ingall, E. D., R. M. Bustin, and P. Van Cappellen.** 1993. Influence of water column anoxia on the burial and preservation of carbon and phosphorus in marine shales. Geochim. Cosmochim. Acta **57:**303–316.
25. **Irgens, R. L., J. J. Gosink, and J. T. Staley.** 1996. *Polaromonas vacuolata* gen. nov., sp. nov., a psychrophilic, marine, gas vacuolate bacterium from Antarctica. Int. J. Syst. Bacteriol. **46:**822–826.
26. **Jia, Z., and R. Conrad.** 2009. Bacteria rather than Archaea dominate microbial ammonia oxidation in an agricultural soil. Environ. Microbiol. **11:**1658–1671.
27. **Kähler, P., and W. Koeve.** 2001. Marine dissolved organic matter: can its C:N ratio explain carbon overconsumption? Deep-Sea Res. Part 1 Oceanogr. Res. Pap. **48:**49–62.
28. **Kaštovská, K., et al.** 2007. Microbial community structure and ecology of subglacial sediments in two polythermal Svalbard glaciers characterized by epifluorescence microscopy and PLFA. Polar Biol. **30:**277–287.
29. **Kirschvink, J. L.** 1992. Late Proterozoic low-latitude global glaciation: the snowball Earth, p. 51–52. *In* J. W. Schopf, C. Klein, and D. Des Maris (ed.), The Proterozoic biosphere: a multidisciplinary study, vol. 2. Cambridge University Press, Cambridge, United Kingdom.
30. **Konneke, M., et al.** 2005. Isolation of an autotrophic ammonia-oxidizing marine archaeon. Nature **437:**543–546.
31. **Larkin, M. A., et al.** 2007. Clustal W and Clustal X version 2.0. Bioinformatics **23:**2947–2948.
32. **Leininger, S., et al.** 2006. Archaea predominate among ammonia-oxidizing prokaryotes in soils. Nature **442:**806–809.
33. **Malhi, S. S., and W. B. McGill.** 1982. Nitrification in three Alberta soils: effect of temperature, moisture, and substrate concentration. Soil Biol. Biochem. **14:**393–399.
34. **Martens-Habbena, W., P. M. Berube, H. Urakawa, J. R. de la Torre, and D. A. Stahl.** 2009. Ammonia oxidation kinetics determine niche separation of nitrifying Archaea and Bacteria. Nature **461:**976–979.
35. **McMechan, M. E.** 1988. Geology of Peter Lougheed Provincial Park, Rocky Mountain Frontier Ranges, Alberta. Open file report 2057. Geological Survey of Canada, Ottawa, Canada.
36. **Mincer, T. J., et al.** 2007. Quantitative distribution of presumptive archaeal and bacterial nitrifiers in Monterey Bay and the North Pacific subtropical gyre. Environ. Microbiol. **9:**1162–1175.
37. **Miteva, V., T. Sowers, and J. Brenchley.** 2007. Production of N_2O by ammonia oxidizing bacteria at subfreezing temperatures as a model for assessing the N_2O anomalies in the Vostok Ice Core. Geomicrob. J. **24:**451–459.
38. **Mosier, A. C., and C. A. Francis.** 2008. Relative abundance and diversity of ammonia-oxidizing archaea and bacteria in the San Francisco Bay estuary. Environ. Microbiol. **10:**3002–3016.
39. **Nicol, G. W., S. Leininger, C. Schleper, and J. I. Prosser.** 2008. The influence of soil pH on the diversity, abundance and transcriptional activity of ammonia oxidizing archaea and bacteria. Environ. Microbiol. **10:**2966–2978.
40. **Norton, J. M., J. M. Low, and M. G. Klotz.** 1996. The gene encoding ammonia monooxygenase subunit A exists in three nearly identical copies in *Nitrosospira* sp. NpAV. FEMS Microbiol. Lett. **139:**181–188.
41. **Okano, Y., et al.** 2004. Application of real-time PCR to study effects of ammonium on population size of ammonia-oxidizing bacteria in soil. Appl. Environ. Microbiol. **70:**1008–1016.
42. **Philippot, L.** 2002. Denitrifying genes in bacterial and archaeal genomes. Biochim. Biophys. Acta **1577:**355–376.
43. **Philippot, L., S. Piutti, F. Martin-Laurent, S. Hallet, and J. C. Germon.** 2002. Molecular analysis of the nitrate-reducing community from unplanted and maize-planted soils. Appl. Environ. Microbiol. **68:**6121–6128.
44. **Potter, L., H. Angove, D. Richardson, and J. Cole.** 2001. Nitrate reduction in the periplasm of gram-negative bacteria. Adv. Microb. Physiol. **45:**51–112.
45. **Rotthauwe, J.-H., L.-P. Witzel, and W. Liesack.** 1997. The ammonia monooxygenase structural gene amoA as a functional marker: molecular fine-scale analysis of natural ammonia-oxidizing populations. Appl. Environ. Microbiol. **63:**4704–4712.
46. **Schloss, P. D., and J. Handelsman.** 2005. Introducing DOTUR, a computer program for defining operational taxonomic units and estimating species richness. Appl. Environ. Microbiol. **71:**1501–1506.
47. **Sharp, M., R. A. Creaser, and M. Skidmore.** 2002. Strontium isotope composition of runoff from a glaciated carbonate terrain. Geochim. Cosmochim. Acta **66:**595–614.
48. **Sharp, M., et al.** 1999. Widespread bacterial populations at glacier beds and their relationship to rock weathering and carbon cycling. Geology **27:**107–110.
49. **Sizova, M., and N. Panikov.** 2007. *Polaromonas hydrogenivorans* sp. nov., a psychrotolerant hydrogen-oxidizing bacterium from Alaskan soil. Int. J. Syst. Evol. Microbiol. **57:**616–619.
50. **Skidmore, M., S. P. Anderson, M. Sharp, J. Foght, and B. D. Lanoil.** 2005. Comparison of microbial community compositions of two subglacial environments reveals a possible role for microbes in chemical weathering processes Appl. Environ. Microbiol. **71:**6986–6997.
51. **Skidmore, M. L., J. M. Foght, and M. J. Sharp.** 2000. Microbial life beneath a high arctic glacier. Appl. Environ. Microbiol. **66:**3214–3220.
52. **Smith, C. J., D. B. Nedwell, L. F. Dong, and A. M. Osborn.** 2007. Diversity and abundance of nitrate reductase genes (*narG* and *napA*), nitrite reductase genes (*nirS* and *nrfA*), and their transcripts in estuarine sediments. Appl. Environ. Microbiol. **73:**3612–3622.
53. **Sørensen, J.** 1978. Denitrification rates in a marine sediment as measured by the acetylene inhibition technique. Appl. Environ. Microbiol. **36:**139–143.
54. **Statham, P. J., M. Skidmore, and M. Tranter.** 2008. Inputs of glacially derived dissolved and colloidal iron to the coastal ocean and implications for primary productivity. Global Biogeochem. Cycles **22:**GB3013.
55. **Stewart, W. D., G. P. Fitzgerald, and R. H. Burris.** 1967. In situ studies on N_2 fixation using the acetylene reduction technique. Proc. Natl. Acad. Sci. U. S. A. **58:**2071–2078.
56. **Stibal, M., M. Tranter, L. G. Benning, and J. R. Rehák.** 2008. Microbial primary production on an Arctic glacier is insignificant in comparison with allochthonous organic carbon input. Environ. Microbiol. **10:**2172–2178.
57. **Tamura, K., J. Dudley, M. Nei, and S. Kumar.** 2007. MEGA4: molecular evolutionary genetics analysis (MEGA) software version 4.0. Mol. Biol. Evol. **24:**1596–1599.
58. **Tranter, M., et al.** 2002. Geochemical weathering at the bed of Haut Glacier d'Arolla, Switzerland—a new model. Hydrol. Proc. **16:**959–993.
59. **Treusch, A. H., et al.** 2005. Novel genes for nitrite reductase and Amo-related proteins indicate a role of uncultivated mesophilic crearchaeota in nitrogen cycling. Environ. Microbiol. **7:**1985–1995.
60. **Wadham, J. L., M. Tranter, S. Tulaczyk, and M. Sharp.** 2008. Subglacial methanogenesis: A potential climatic amplifier? Global Biogeochem. Cycles **22:**GB2021.
61. **Wuchter, C., et al.** 2006. Archaeal nitrification in the ocean. Proc. Natl. Acad. Sci. U. S. A. **103:**12317–12322.
62. **Wynn, P. M., A. J. Hodson, T. H. E. Heaton, and S. R. Chenery.** 2007. Nitrate production beneath a High Arctic glacier, Svalbard. Chem. Geol. **244:**88–102.
63. **Yergeau, E., H. Hogues, L. G. Whyte, and C. W. Greer.** 2010. The functional potential of high Arctic permafrost revealed by metagenomic sequencing, qPCR and microarray analyses. ISME J. **4:**1206–1214.
64. **Zehr, J. P., B. D. Jenkins, S. M. Short, and G. F. Steward.** 2003. Nitrogenase gene diversity and microbial community structure: a cross-system comparison. Environ. Microbiol. **5:**539–554.
65. **Zhang, L.-M., M. Wang, J. I. Prosser, Y.-M. Zheng, and J.-Z. He.** 2009. Altitude ammonia-oxidizing bacteria and archaea in soils of Mount Everest. FEMS Microbiol. Ecol. **70:**208–217.
66. **Zumft, W. G.** 1997. Cell biology and molecular basis of denitrification. Microbiol. Mol. Biol. Rev. **61:**533–616.